Journal of Power Sources 262 (2014) 245–254

Contents lists available at ScienceDirect

Journal of Power Sources

journal homepage: www.elsevier.com/locate/jpowsour

A novel approach to the experimental study on methane/steam reforming kinetics using the Orthogonal Least Squares method

Anna Sciazko [a,b,*], Yosuke Komatsu [b], Grzegorz Brus [a], Shinji Kimijima [c], Janusz S. Szmyd [a]

[a] AGH University of Science and Technology, Faculty of Energy and Fuels, Department of Fundamental Research in Energy Engineering, 30 Mickiewicza Ave., 30-059 Krakow, Poland
[b] Shibaura Institute of Technology, Graduate School of Engineering, Division of Regional Environment Systems, 307 Fukasaku, Minuma-ku, Saitama-shi, 337-8570 Saitama, Japan
[c] Shibaura Institute of Technology, College of Systems Engineering and Science, Department of Machinery and Control Systems, 307 Fukasaku, Minuma-ku, Saitama-shi, 337-8570 Saitama, Japan

HIGHLIGHTS

- Deriving reaction kinetics of the methane/steam reforming process on Ni/YSZ cermet.
- An implementation of the Generalized Least Squares (GLS) method to the calculation.
- Determining the most probable values of the empirical parameters.
- *A posteriori* evaluation of the errors of directly measured and unknown variables.
- GLS method is useful in securing higher accuracy of results and measured data.

ARTICLE INFO

Article history:
Received 14 January 2014
Received in revised form
22 February 2014
Accepted 20 March 2014
Available online 28 March 2014

Keywords:
Methane/steam reforming
Generalized Least Squares method
Uncertainty analysis
Ni/YSZ catalyst

ABSTRACT

For a mathematical model based on the result of physical measurements, it becomes possible to determine their influence on the final solution and its accuracy. However, in classical approaches, the influence of different model simplifications on the reliability of the obtained results are usually not comprehensively discussed. This paper presents a novel approach to the study of methane/steam reforming kinetics based on an advanced methodology called the Orthogonal Least Squares method. The kinetics of the reforming process published earlier are divergent among themselves. To obtain the most probable values of kinetic parameters and enable direct and objective model verification, an appropriate calculation procedure needs to be proposed. The applied Generalized Least Squares (GLS) method includes all the experimental results into the mathematical model which becomes internally contradicted, as the number of equations is greater than number of unknown variables. The GLS method is adopted to select the most probable values of results and simultaneously determine the uncertainty coupled with all the variables in the system. In this paper, the evaluation of the reaction rate after the pre-determination of the reaction rate, which was made by preliminary calculation based on the obtained experimental results over a Nickel/Yttria-stabilized Zirconia catalyst, was performed.

1. Introduction

The methane/steam reforming process, often used for the synthesis gas (syngas) production from hydrocarbon source, is one of the fuel conversion methods, which are especially important in the context of high temperature fuel cells such as Solid Oxide Fuel Cells (SOFCs). This technology is beneficial for power generation in SOFCs, considering their fuel flexibility [1].

The high operating temperature of the cell eliminates the necessity of the external heat source for the strongly endothermic reforming reaction. Regarding this advantage, coupling of the reforming process with SOFCs is a beneficial solution for hydrogen production in fuel cell technology. To properly address and implement this technique to the technological development of SOFCs, the

* Corresponding author. Shibaura Institute of Technology, Graduate School of Engineering, Division of Regional Environment Systems, 307 Fukasaku, Minuma-ku, Saitama-shi, 337-8570 Saitama, Japan. Tel.: +81 48 687 5174; fax: +81 48 687 5197.
E-mail addresses: xz13005@sic.shibaura-it.ac.jp, sciazko@agh.edu.pl (A. Sciazko).

http://dx.doi.org/10.1016/j.jpowsour.2014.03.097
0378-7753/

implementation of an internal reforming system, modelling and numerical analyses of the phenomena occurring inside the SOFC systems are important subjects. The reason relies on the fact that the fuel reforming process, in particular the designing and optimizing of an indirect internal reformer and a cell with direct reforming for an SOFC application, involve problems connected with heat transfer phenomena in porous media. To conduct numerical modelling, proper kinetics of the reaction is also needed to improve the reliability of numerical modelling. Thus, the treatment of reaction kinetics and physical phenomena in a system are very important subjects to be accomplished.

The kinetics of the reforming process can be described by one of three concepts: i) General Langmuir–Hinshelwood kinetics, ii) first order reaction with respect to methane and iii) power law expressions derived from data fitting [2–5]. One of commonly used mathematical expressions of the methane/steam reforming reaction is determined as the reaction rate: $r_{CH_4} = k(p_{CH_4})^a(p_{H_2O})^b$, by taking the advantage of the power law expression. The reaction rate of the reforming reaction is very sensitive on the catalytic activity, reaction temperature and the partial pressure of the reactants. Thus, the investigation relies on the material properties and transport phenomena. To find out the proper reaction kinetics, the preparation of the sample and experimental conditions are very important concerns to clarify the reaction kinetics.

There are many studies focusing on the kinetics of methane/steam reforming [2–16]. The experimental investigation has been also done over the Nickel/Yttria-Stabilized Zirconia (Ni/YSZ), which is a popularly adopted SOFC anode material [2,3,6–13,15,16]. As seen in Refs. [2,3,6–13,15,16], the derived empirical parameters describing the process reported in them are divergent among themselves. For instance, Table 1 shows one of empirical parameters, the so-called reaction order a and b found in the literatures [2,7,9–13,15,16]. Although, the empirical parameters a and b should be independent from the specific property of the investigated sample, as far as the same type of catalyst is used [9]. Moreover, uncertainties of the obtained result, which may have influenced the derived reaction kinetics, were not substantially discussed in the published investigations. Thus, this paper presents a new approach to the analysis of the reforming process, introducing a numerical procedure incorporating the Generalized Least Squares (GLS) method.

The conventional methods of modelling multi-physical phenomena involving (heat and mass) transport problems usually describe analysed systems with a set of equations, which are uniquely defined in the mathematical sense. In general, this type of theoretical approach yields unique solutions from the peculiarly specified constraints set of equation for a system. Besides, they assume that each variable or model parameter is precisely defined and their uncertainties are negligible (Fig. 1(a)). However, in the case of the methane/steam reforming process, in which the model parameters include the properties from a general thermodynamic table, the assumption of accuracy of all of those factors can lead to the simplification of the model. The model simplification can also be inducted by an applied mathematical approach both in the phase of definition and during the model solving stage. Moreover, one of the most significant factors in identifying the inaccuracies of the model solutions is connected with the uncertainties of the directly measured variables (observations) incorporated in the problem description (Fig. 1(b)). The model defined in this manner results in the unique description of the phenomena, although the numerical results can differ from the actual state of the system behaviour and the degree of accuracy of the model that is usually difficult to estimate. The present study analyses the concept of most probable value of a theoretical solution and a measure of its inaccuracy. The proposed methodology allows for including additional data directly in the mathematical model of the process as the new (supplementary) variables. A model, which includes supplementary data, contains more equations than unknowns, and because the uncertainties of the directly measured variables (observations) can be internally contradicted. Choosing different subsets of constraint equations allows for the calculation of the unknowns in many, theoretically correct ways and a problem, which arises, is how to determine the most probable result. The GLS procedure is proposed as a method of correcting the measured data, securing its higher accuracy and obtaining the most probable value and its uncertainty for the parameters to be determined by numerical computation (Fig. 1(c)). Additionally, it can be noted that the GLS method provides the objective criteria for the formal evaluation and falsification of different mathematical models of investigated phenomena.

The present paper introduces a novel approach to derive reaction kinetics described by a power law type of equation. The effect of uncertainties on the derived reaction rate is primarily discussed by adopting the GLS method. This approach leads to improving the reliability of the derived reaction kinetics of the methane/steam reforming process. The challenge to conclude the applicability of the GLS method in the analysis of the chemical reaction process is also highlighted in this paper.

Table 1
Comparison of the reaction kinetics parameter, reaction orders a and b, found in literatures.

Reference	a	b
Brus [2]	0.98	−0.09
Ahmed and Foger [7]	0.85	−0.35
Iwai et al. [9]	0.82	0.14
King et al. [10]	1	0
Lee et al. [11]	1	−1.25
Odegard et al. [12]	1.2	0
Timmermann et al. [13]	1.19	0
Yakabe et al. [15]	1.3	−1.2
Mogensen [16]	0.7	0

2. Computational method

The classical approach to mathematical modelling assumes that real life problems can be described and defined by a finite set of mathematical equations. In general, the problem with N unknowns and K measured values can be solved unambiguously when there are N equations in the mathematical model. However, in many theoretical approaches, the uncertainties created by model simplifications and experimental errors cause the unknown uncertainty of the obtained solution. On the other hand, when the number of equations exceeds the number of unknowns (a set of overdetermined equations) and the measured values are characterized by experimental errors, the model equation set becomes internally contradicted. The Least Squares (LS) method provides a strategy for finding the approximate and most probable solution of an overdetermined system of equations. The first comprehensive formulation of the least squares (LS) method, was presented by Legendre's in 1805 [17]. Initially, the LS method was used mainly in geodetic calculations and then Sweneker, who investigated the balances of substances in the branched pipelines, presented its first application to the energy science problem [18]. The application to the energy science and the theoretical aspects of the LS method were developed [19–26]. The research involved problems connected with theory of coordination of material and energy balance [19–21], heat transfer by convection and radiation and the prediction of temperature distribution [22,23]. Other concerned issues were investigations related to carbon dioxide emissivity [24],

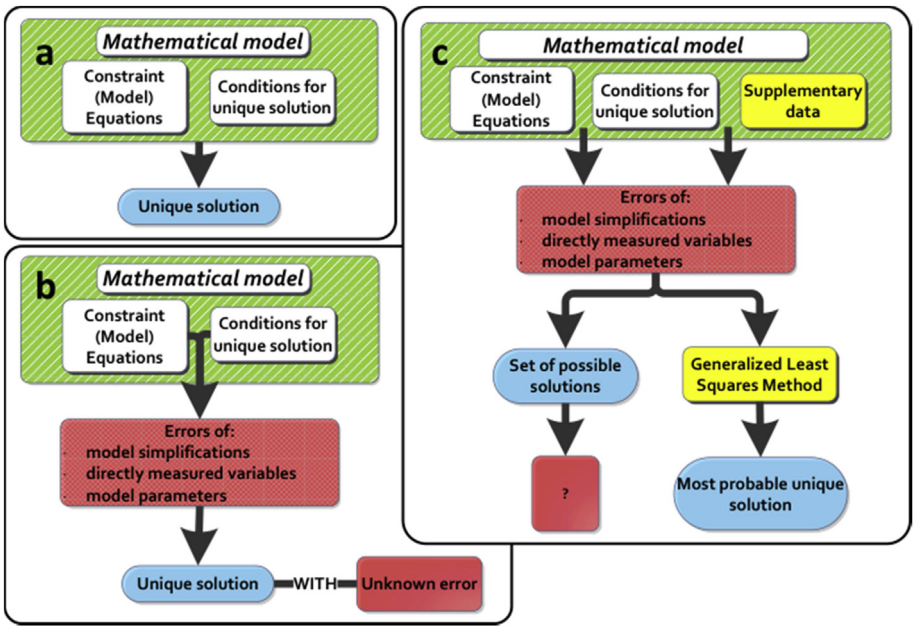

Fig. 1. Approaches to mathematical modelling: (a) classical problem definition, (b) errors of mathematical models and (c) models with supplementary data.

solidification of binary alloys [25], and modelling of the autocatalytic reactions [26].

2.1. Least squares method

Mathematical models describing real process are usually defined by nonlinear equation sets consisting of algebraic functions and differential equations. First, assume that the considered problem is described by a set of J algebraic equations:

$$f_j\left(u^*,x^*\right)=0,\quad (j=1,2,\cdots,\mathrm{J}),\quad u^*=\begin{pmatrix}u_1^*\\u_2^*\\\vdots\\u_{\mathrm{K}}^*\end{pmatrix}\quad\text{and}\quad x^*=\begin{pmatrix}x_1^*\\x_2^*\\\vdots\\x_{\mathrm{N}}^*\end{pmatrix}\tag{1}$$

where $\mathbf{u}^*$ is K-elements vector of the quantities to be measured and $\mathbf{x}^*$ is N-elements vector of the quantities to be solved by numerical computation. Although for measured values $\mathbf{u}$ and approximations of unknowns $\mathbf{x}$ the equation set is not precisely fulfilled:

$$f_j(u,x)=-w_j,\quad (j=1,2,\cdots,J),u=\begin{pmatrix}u_1\\u_2\\\vdots\\u_{\mathrm{K}}\end{pmatrix}\quad\text{and}\quad x=\begin{pmatrix}x_1\\x_2\\\vdots\\x_{\mathrm{N}}\end{pmatrix}\tag{2}$$

where w_j designates the residual of the j-th equation. Real values $\mathbf{u}^*$ and $\mathbf{x}^*$ are sums of measurements and approximations of unknowns ($\mathbf{u}$ and $\mathbf{x}$) and corrections ($\mathbf{v}$ and $\mathbf{y}$): $\mathbf{u}^*=\mathbf{u}+\mathbf{v}$ and $\mathbf{x}^*=\mathbf{x}+\mathbf{y}$. Therefore it can be written:

$$f_j(u+v,x+y)=0,\quad (j=1,2,\cdots,J),\quad v=\begin{pmatrix}v_1\\v_2\\\vdots\\v_{\mathrm{K}}\end{pmatrix}\quad\text{and}\quad y=\begin{pmatrix}y_1\\y_2\\\vdots\\y_{\mathrm{N}}\end{pmatrix}\tag{3}$$

Moreover, it is assumed that experimental errors s_k of measurements satisfies the normal distribution with mean value equals zero and variances σ_k^2: $s_k \sim N(0,\sigma_k^2)$.

According to assumptions, f_j are the unrestricted algebraic functions. However, the least squares method requires the linear form of the constraint equations. If the f_j functions are differentiable, they can be presented in the form of a Taylor series in the neighbourhood of the point P($\mathbf{u}$,$\mathbf{x}$). The linearization of a function f_j is the first order term of its Taylor expansion around the point of interest. After linearization, the constraint equations can be written in the matrix form:

$$Av+By=w\tag{4}$$

where $\mathbf{A}=df_j/du_k$ is J × K Jacobi's matrix and $\mathbf{B}=df_j/dx_n$ is J × N Jacobi's matrix. The LS method assumes the minimization of the following function:

$$\Phi(v)=v^{\mathrm{T}}C_S^{-1}v=\sum_{k=1}^{\mathrm{K}}\left(\frac{v_k}{\sigma_k}\right)^2\rightarrow\min\tag{5}$$

where $\mathbf{C_S}$ is the covariance matrix with the measurement variances σ_k^2 on the diagonal and 0 on the other positions (due to the independence of the variables). The method of Lagrange multipliers is applied in order to achieve the extreme and find corrections:

$$\begin{aligned}y&=G^{-1}B^{\mathrm{T}}F^{-1}w\\v&=C_sA^{\mathrm{T}}F^{-1}(w-By)\end{aligned}\tag{6}$$

where $\mathbf{F}=\mathbf{AC_SA}^{\mathrm{T}}$ and $\mathbf{G}=\mathbf{B}^{\mathrm{T}}\mathbf{F}^{-1}\mathbf{B}$.

2.2. Generalized Least Squares method

The Generalized Least Squares (GLS) method (Unified Least Squares Method) was introduced by Mikhail and Ackermann [27]. The classical definition of the least squares method assumes that the rank of matrix $\mathbf{A}$ is equal to the amount of model equations J. In many problems this assumption is not fulfilled because the number of equations f_j is different than the amount of measured values u_k.

Thus, Eq. (6) proposed in the classical method cannot be used because the matrix $\mathbf{F}^{-1}$ does not exist.

The most important assumption of the GLS method is that all model variables (measured values **u** and unknowns **x**) are observations and treated numerically in the same manner. The only difference between them is the assumption that errors of unknowns are much bigger than the errors of measured values ($s_k \gg s_n$).

After the linearization of the model equations the constraints can be written:

$$A_B V_B = W_B \tag{7}$$

where $\mathbf{A_B} = [\mathbf{AB}]$and $\mathbf{V_B} = [\mathbf{vy}]^T$ and then the covariance matrix has the following form:

$$C_B = \begin{bmatrix} C_S & 0 \\ 0 & C_{SX} \end{bmatrix} \tag{8}$$

where $\mathbf{C_S}$ and $\mathbf{C_{SX}}$ are the covariance matrices with diagonals consisting of variances of measurements σ_k^2 and unknowns σ_n^2 respectively. To solve the GLS problem and minimize the function $\Phi(\mathbf{v},\mathbf{y})$, which has the following form:

$$\Phi(v,y) = \sum_{k=1}^{K} \left(\frac{v_k}{s_k}\right)^2 + \sum_{n=1}^{N} \left(\frac{y_n}{s_n}\right)^2 \rightarrow \min \tag{9}$$

the Lagrange multiplier method is used and it gives the solution:

$$\mathbf{V_B} = \mathbf{C_B A_B^T F_B^{-1} W_B}, \quad \text{where} \quad \mathbf{F_B} = \mathbf{A_B C_B A_B^T} \tag{10}$$

2.3. Errors of solution

To yield new error bounds for corrected measured data ($\mathbf{u}$, $\mathbf{C_U}$) and the theoretically solved variables ($\mathbf{x}$, $\mathbf{C_X}$), the law of error propagation can be applied. The new covariance matrices for the classical LS method can be written:

$$\begin{aligned} C_U &= C_S - SAC_S \\ C_X &= \left(B^T T^{-1} B\right)^{-1} \end{aligned} \tag{11}$$

where $\mathbf{S} = \mathbf{C_S A^T F^{-1}(I - BG^{-1}B^T F^{-1})}$ and **I** is the unit matrix.

On the other hand, in the case of the generalized approach, the calculated covariance matrix of improved observations has the following form:

$$C_{VB} = C_B - C_B A_B^T F_B^{-1} A_B C_B = \begin{bmatrix} C_U & C_{UX} \\ C_{UX}^T & C_X \end{bmatrix} \tag{12}$$

2.4. Interpretation of the covariance matrix

The covariance matrix $\mathbf{C_{VB}}$ defined by Kolenda et al. [25] represents the hyperellipsoid of the (K + N)-dimensional normal distribution. The covariance ellipsoid is the hypersurface in the (K + N)-dimensional space and is always inside the (K + N)-dimensional cuboid defined by the central point $P'(\mathbf{u}^*,\mathbf{x}^*)$ and the square roots of the diagonal elements of $\mathbf{C_{VB}}$ which represent the lengths of the cuboid edges. Covariance hyperellipsoid touches cubicoid in 2(K + N) points and its volume can be calculated from the formula:

$$V_{K+N} = \frac{\sqrt{(K+N+2)\pi^{(K+N+2)}|C_{VB}|}}{\Gamma\left(\frac{1}{2}(K+N)+1\right)} \tag{13}$$

where Γ is the Euler's gamma function.

Generally, it can be noted that the lines of constant probability are ellipsoids similar to the covariance ellipsoid. Those ellipsoids are situated inside (outside) of it for larger (smaller) probability. For the largest probability the ellipsoid collapses to the central point [28]. Thus, it can be pointed out that conditions for achieving the global minimum can be presented equivalently as the minimization of the hyperellipsoid's volume and the minimization of the covariance matrix's determinant:

$$\min(V_{K+N}) \rightarrow \min(|C_{VB}|) \text{or} \ \min\left[\frac{1}{K+N}\left(\sum_{k=1}^{K}\sigma_k^2 + \sum_{n=1}^{N}\sigma_n^2\right)\right] \tag{14}$$

The presented formula can be used for the falsification of different mathematical models describing the examined physical phenomena.

3. Experimental studies on methane/steam reforming

The analysis of the reforming process was coupled with the experimentation of methane/steam reforming reaction kinetics derived over a Nickel/Yttria-Stabilized Zirconia catalyst material (NiO/YSZ 60:40 vol%, AGC SEIMI CHEMICAL CO. LTD [29]. The Ni/YSZ cermet is chosen for the anode of SOFCs, because this material satisfies the following criteria of requirements: inexpensive fabrication cost, high electrical conductivity, high electrocatalytic activity, stability under reducing environment, thermal expansion and chemical compatibility with other materials composing the SOFC cell layers and ensuring sufficient Three Phase Boundary (TPB) for the electrochemical process [30–33]. Moreover, a lot of studies on the reaction kinetics of the methane/steam reforming reaction over the Ni/YSZ catalyst were published earlier and huge inconstancies were found in them as preceded in the introduction. Thus, the main goal of the present work is to evaluate the effect of acceptable inaccuracies (caused by the specificity of measurements) on the reforming performance in the form of the rate equation, which is dependent on the empirical parameters. To satisfy the objectives, the combined experimental-numerical methodology proposed by Odegard [12] and modified by Brus et al. [8] was applied.

Fig. 2(a) shows the schema of the experimental setup. Three main parts of the system can be noted: the inlet part, where the substrate gases are prepared, the reaction part with the reformer tube placed in the furnace and the outlet part where the product of the reforming reaction is analysed.

The experiment was performed with high purity methane (CH_4) supplied from a gas cylinder via the mass flow controller and water (H_2O) fed with the pump. Additionally, nitrogen (N_2) was also supplied to the reactor to maintain the reforming conversion rate at a low level and to enable to derive the correct reforming kinetics equation, since the reaction has to occur in the entire volume of catalyst. N_2 does not have a direct influence on the occurring reactions but changes the partial pressures of the components and finally decreases the methane conversion rate. Thus, the gas mixture of CH_4, N_2 and H_2O was supplied to the reaction zone. CH_4 was regulated 200 [kPa] and supplied with the mass flow controller, N_2 was and also treated in the same way. H_2O was pumped and supplied to the evaporator, which is used at the same time as the preheater for heating the gas mixture.

The main part of the system is the stainless steel reformer of which the schema is presented in Fig. 2(b). In the experimental investigation the Nickel/Yttria-Stabilized Zirconia catalyst in the form of fine quality powder of NiO/YSZ, of which the composition is 60:40 in volume ratio, was used. The catalyst powder used in the

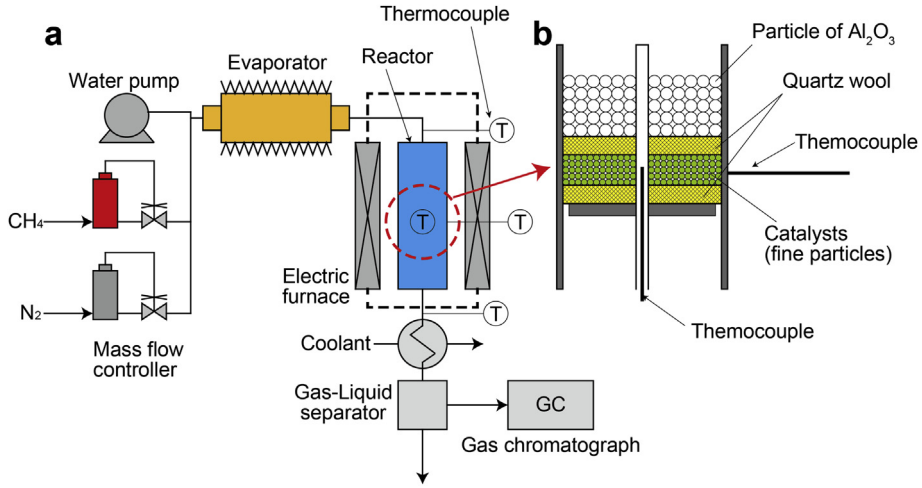

Fig. 2. Schema of (a) experimental setup and (b) reactor.

experiment is spherical in shape and has a 0.85 [μm] diameter with a specific surface area 5.2 [m^2] per 1 [g] of catalyst [29]. The fine powder catalyst was used in order to determine the kinetics of the catalysed methane/steam reforming process without the influence of mass transport process [16]. It is crucial to avoid the mass transfer limitations because they can lower the activity of the catalyst, especially in the case of exponentially fast reactions [11–13,16]. The catalyst, of which the amount used in the experiment was 3 [g], was dispersed to be a homogeneous distribution over the quartz wool-made bed located in the middle of the reactor. Then, the catalyst layer was covered with the quartz wool and then the half upper of the reactor was fulfilled with Al_2O_3 balls. The catalyst is preceded by Al_2O_3 balls used to prevent a cooling effect of the entering fluid and avoid a large temperature gradient in the reformer. The gas mixture reaches the reaction zone with the catalyst after preheating by the electric furnace to the reaction temperature. A reformer tube is placed in the electrical furnace with a maximum temperature of 800 [°C]. The preheater and after-heater allow to reach the maximal temperature of 400 [°C], however, the temperature was set at 200 [°C] for both of them during the experimental procedure. The temperature of the reactor and the temperature around it are controlled with the thermocouples located before and after the furnace as well as by the thermocouples vicinity of the reformer (on the surface and inside reaction zone).

After the reforming reaction the exhaust gas was analysed by the gas chromatograph (GC390B by GL Sciences). The gas supplied to the gas chromatograph was dried by cooling down the gas mixture to 2 [°C] for the preliminary of the chromatography. Two methods of gas detection were used: TCD (Thermal Conductivity Detector) to the methane $m^o_{CH_4}$ and hydrogen $m^o_{H_2}$ and FID (Flame Ionization Detector) with a methanizer for the carbon monoxide m^o_{CO} and carbon dioxide $m^o_{CO_2}$ detection, where m stands for the molar fraction of the chemical species and the superscript o denotes measurements at the outlet.

Before conducting measurements, the catalyst was treated at the evaluated temperature of 800 [oC] with a mixture of 150 [ml min^{-1}] nitrogen and 100 [ml min^{-1}] hydrogen due to the reduction process of NiO. NiO/YSZ had been kept in the reduction process for 6 [h]. The measurements were carried out with different conditions based on the various temperatures (in the range of 550–750 [°C]), Steam-to-Carbon ratio SC (in the range of 2.5–6) and Nitrogen-to-Carbon ratio NC (in the range of 0.5–6). The details of the experimental conditions are shown in Table 2. The other perspective of supplying N_2 was for levelling the residential time of the mixture gas flow at constant among the various flow rate conditions.

4. Analysis

4.1. Preliminary analysis

Methane/steam reforming is the conventional method of hydrogen production and reactions governing this process are following two reactions [12].

Methane/steam reforming reaction:

$$CH_4 + H_2O \rightarrow 3H_2 + CO \tag{15}$$

Shift reaction:

$$CO + H_2O \leftrightarrow H_2 + CO_2 \tag{16}$$

The reaction rate of the methane/steam reforming reaction can be described by the following equations:

$$r = k(p_{CH_4})^a (p_{H_2O})^b$$
$$k = A\exp\left(\frac{-E}{RT}\right) \tag{17}$$

where r is the reaction rate [mol s^{-1} g^{-1}], k is the reaction constant, p_{CH_4} and p_{H_2O} are the partial pressures of CH_4 and H_2O [Pa], a and b are the reaction order coefficients [−], A is the pre-exponential factor [mol g^{-1} s^{-1} $Pa^{-(a+b)}$], E is the activation energy [J mol^{-1}], R is the universal gas constant [J mol^{-1} K^{-1}] and T is the

Table 2
Experimental conditions for different values of SC and NC ratios.

SC [−]	NC [−]	Volume flow rate [ml min^{-1}] CH_4	Volume flow rate [ml min^{-1}] N_2	Volume flow rate [ml min^{-1}] H_2O	Total molar flow rate [mol min^{-1}]
3	3	50	150	0.11	1.43×10^{-2}
2.5	6	37	221	0.07	1.43×10^{-2}
5	4	35	140	0.13	1.43×10^{-2}
4	2	50	100	0.15	1.43×10^{-2}
3	1	70	70	0.15	1.43×10^{-2}
6	0.5	47	23	0.21	1.43×10^{-2}

temperature [K]. On the other hand, the shift reaction is a fast process and reaches equilibrium instantaneously, and therefore it is assumed that its conversion rate can be calculated from the equilibrium equation:

$$K_{\text{shift}} = \frac{p_{H_2} p_{CO_2}}{p_{CO} p_{H_2O}} = \exp\left(\frac{-\Delta G}{RT}\right) \tag{18}$$

where p_{H_2}, p_{CO_2}, p_{CO} and p_{H_2O} are the partial pressures of H_2, CO_2, CO and H_2O [Pa] and ΔG is the change in Gibbs free energy [J mol^{-1}].

The reforming process is defined by the values of the empirical parameters describing the reaction order coefficients a and b, activation energy E, and pre-exponential factor A. To determine their values and the uncertainty of the obtained results the GLS method has been applied. Two main phases of the analysis can be pointed: preliminary calculations to estimate the initial values of the unknown parameters in the vector **x** and the application of the GLS method. The GLS algorithm, which is presented in Fig. 3, started from the determination of the constraint equations describing the problem and definition of the vector that contains measured and unknown variables. The next step was to introduce the covariance matrix containing the uncertainties of all the involved variables. After that, the values of the unknowns were initialized, based on the preliminary calculation. The linearization of the constraint equations with the determination of the Jacobi's matrix and Lagrange multipliers method allowed for the calculation of the correction vectors. In addition, new error bounds for corrected measured data were estimated. The last step was to verify the convergence of the obtained solution and stipulate the criteria of convergence or recalculation on the basis of the unknown values determined in the previous step.

The preliminary calculations were divided into two parts. The first of them was based on the observation that the value of the reaction constant does not depend on the SC and NC ratios [12]. The computation was fist conducted to derive the reaction orders, a and b, with the carefully designed experimental conditions. Moreover, the SC and NC ratios characterizing the experimental conditions were widely and properly dispersed to minimize the influence of the possible measurement uncertainties. Different combinations of the parameters a (range 0–1.5) and b (range −0.5–0.5) were tested and the calculated reaction constants were compared with the experimental results from the conditions (Table 2), at which widely dispersed SC and NC ratios were applied. The range of parameters a and b was chosen in accordance with published data [8,10,12]. The experimental conditions were set to keep the total inlet flow rate at a constant level. For each computation conducted for different experimental conditions, the parameters a and b with results showing the smallest standard deviation from k were selected. The relative standard deviation RSD_k is expressed as follows:

$$\text{RSD}_k = \frac{\sqrt{\sum_{j=1}^{n} (k_i - k_{\text{ave}})^2}}{n \cdot k_{\text{ave}}} \quad (i = 1, 2, \cdots, n) \tag{19}$$

where, n and k_{ave} stand for the number of measurements and average of the reaction constant k at each temperature condition, respectively. In this stage, the reaction constant k was derived by the following observation: the non-equilibrium reaction for the plug-flow reactor rate can be described as a ratio between the change in the flow rate of methane and the change in the amount of catalyst [34]. Mathematically, the reaction rate of the steam reforming reaction can be described as:

$$r = \frac{-\mathrm{d}F_{CH_4}}{\mathrm{d}w_{\text{cat}}} \tag{20}$$

where, $F_{CH_4} = F^i_{CH_4} \cdot (1 - x)$, $F^i_{CH_4}$ is the methane flow rate [mol s^{-1}] and one at the inlet and of the catalyst layer, x is the dimensionless converted amount of methane in the catalyst layer, and w_{cat} is the weight [g] of catalyst. By combining Eqs. (17) and (20), the reaction constant k is given as the following formula:

$$k = \left(\frac{F^i{}_{CH_4}}{w_{\text{cat}}}\right) \cdot \int \left[\frac{1}{(p_{CH_4})^a (p_{H_2O})^b}\right] \cdot \mathrm{d}x \tag{21}$$

From the stoichiometry of the reaction [15] and [16], the partial pressures can be defined as:

$$p_{CH_4} = \left(\frac{F_{CH_4}}{F_{\text{all}}}\right) \cdot P = \frac{1 - x}{1 + SC + NC + 2x} \cdot P \tag{22}$$

$$p_{H_2O} = \left(\frac{F_{H_2O}}{F_{\text{all}}}\right) \cdot P = \frac{SC - x - y}{1 + SC + NC + 2x} \cdot P \tag{23}$$

where, F_{all} is the total amount of product [mol s^{-1}] at the outlet of the reactor, P is the total pressure [Pa], F_{CH_4}, F_{H_2O} are, respectively, the amount of CH_4 and steam in [mol s^{-1}] at the reformer output and y is a fraction of reacted carbon monoxide. Introducing Eqs. (22) and (23) into Eq. (21), the final formulation of the reaction constant becomes as following:

$$k = \left(\frac{F^i_{CH_4}}{w_{\text{cat}}}\right) \cdot \int_0^{x_{\text{out}}} \left[\frac{(1 + SC + NC + 2x)^{a+b}}{P^{a+b}(1 - x)^a (SC - x - y)^b}\right] \cdot \mathrm{d}x \tag{24}$$

where a and b are coefficients related to the reaction order. The methane conversion rate x, which was used to introduced to Eq. (24), is determined by the outlet quantity of CH_4, CO and CO_2 and expressed as [35]:

$$x = \frac{m^o_{CO} + m^o_{CO_2}}{m^o_{CH_4} + m^o_{CO} + m^o_{CO_2}} \tag{25}$$

where, $m^o_{CH_4}$, m^o_{CO}, $m^o_{CO_2}$ is the mole fraction of CH_4 and CO and CO_2 at the outlet of the reactor. The values $a = 0.97$ [−] and $b = -0.08$ [−] were characterized by the smallest summed standard deviation and chosen as the best description of the process (Fig. 4).

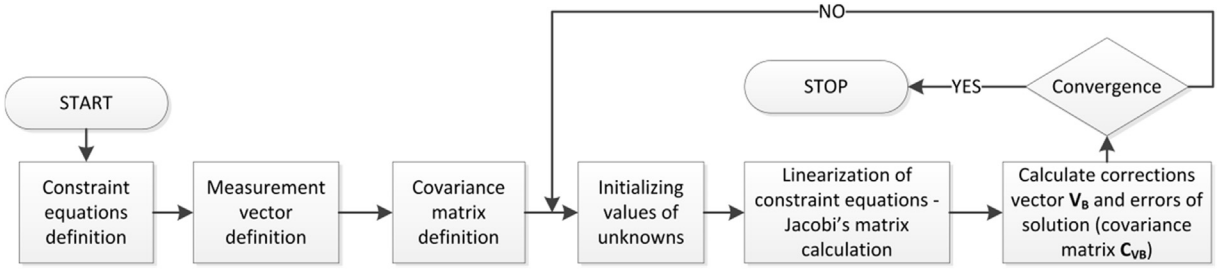

Fig. 3. GLS algorithm diagram.

The next stage was the preparation of the Arrhenius plot based on the data obtained from the experiments carried out in different temperatures (550–750 [°C]). The approximation line (Fig. 5):

$$\ln k = \ln A - \frac{E}{R}\cdot\frac{1}{T} \tag{26}$$

was used to find the values of the activation energy $E = 117.219 \times 10^3$ [J mol^{-1}] and the pre-exponential factor $A = 1.554 \times 10^{-3}$ [mol g^{-1} s^{-1} Pa$^{-0.89}$]. Thus, the first approximation of the kinetic equation of the methane/steam reforming reaction can be written as:

$$R_{st} = w_{cat}\cdot r = w_{cat}\cdot 1.554\times 10^{-3} \cdot\exp\left(\frac{-117\times 10^3}{RT}\right)(p_{CH_4})^{0.97}(p_{H_2O})^{-0.08} \tag{27}$$

where, w_{cat} stands for the weight of a catalyst [g] and the subscript *st* denotes for the steam reforming. Fig. 6(a) shows the representative examples of conversion rates obtained from the experiment. The one of the most important factors in deriving the proper non-equilibrium kinetic equation are the adequate experimental conditions which ensure the conversion rate and reaction rate are not following the equilibrium reaction. This can be achieved by choosing the appropriate amount of catalyst and flow rates of the reaction substrates. Fig. 6(b) and (c) represent Gas Hourly Space Velocity (GHSV) connecting to both of those factors in correlation with achieved conversion rates. The GHSV is described as the function of the mixture gas velocity $\dot{V}_{gas}$ [mm^3 h^{-1}] and the volume of the catalyst layer V_{cat} [mm^3]:

$$\mathrm{GHSV} = \frac{\dot{V}_{gas}}{V_{cat}} \tag{28}$$

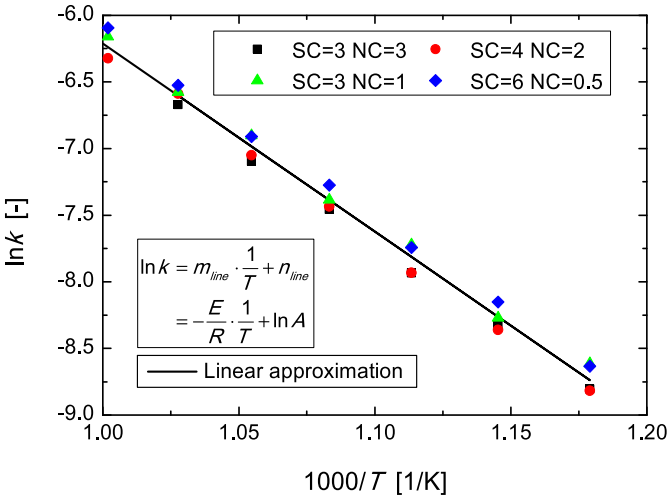

Fig. 5. Arrhenius plot for Ni/YSZ.

Fig. 6(b) is the case where the SC and NC ratios are fixed at 3 for each of them. In the meantime, Fig. 6(c) is the case where the temperature is fixed at 700[°C]. It can be noted that for small GHSV values (small amount of gas in high amount of the catalyst), the achieved conversion rate are high, which means that the reaction is very close to equilibrium and is not proper for delivering kinetic equation. On the other hand, for big GHSV values the changes in obtained conversion rates are very small and difficult to observe. For kinetic consideration the best are moderate values of GHSV, which results in moderate conversion rates for different observed temperatures and SC and NC conditions.

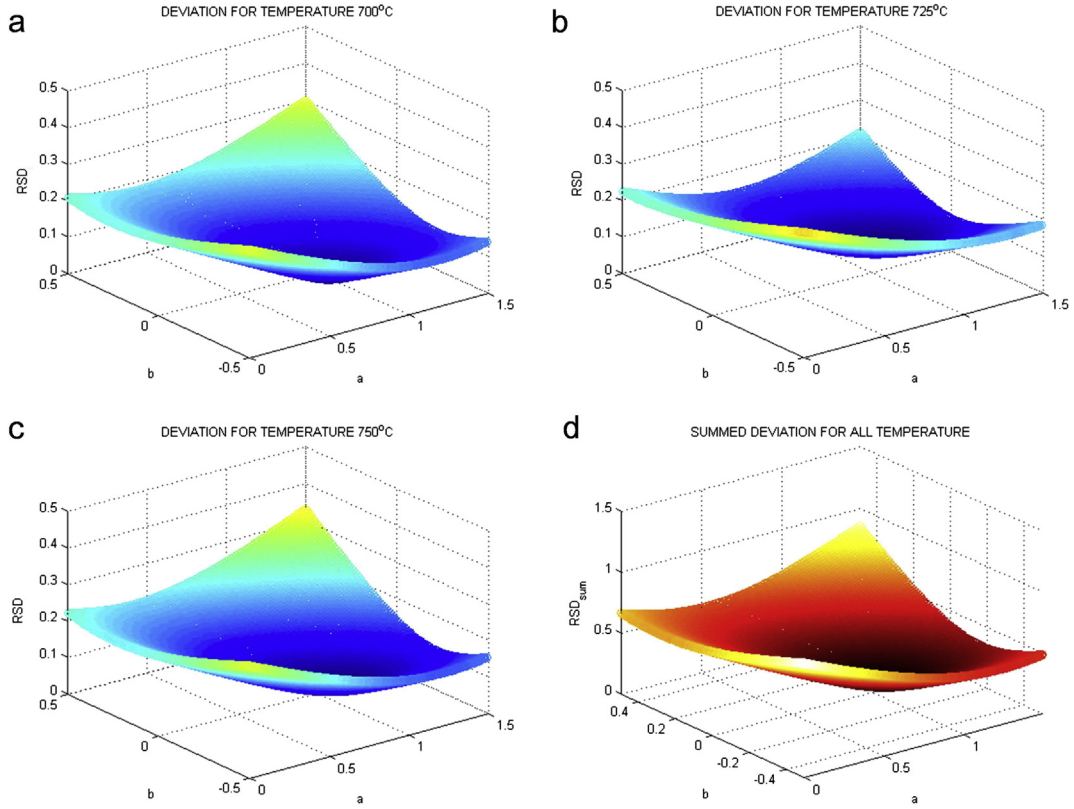

Fig. 4. Preliminary calculations of the process parameters: analysis of the relative standard deviation (RSD) of the value of reaction constant at the reaction temperature of (a) 700, (b) 725 and (c) 750 [°C] and (d) the sum of the Relative Standard Deviation (RSD_{sum}) with different values of parameters of reaction orders *a* and *b*.

4.2. Analysis with the application of the GLS method

The constraint equations used in the GLS algorithm to describe the process of methane reforming can be divided into three basic groups: the kinetic reforming equation (29), the linear Arrhenius equation (30) and the balances of the basic chemical elements: carbon, hydrogen, oxygen and nitrogen in Eqs. (31)–(34):

$$\frac{F_{CH_4}^{i(j)} - F_{CH_4}^{o(j)}}{w^{(j)}} - A \cdot \exp\left(\frac{-E}{RT^{(j)}}\right)\left(p_{CH_4}^{(j)}\right)^a \left(p_{H_2O}^{(j)}\right)^b = 0 \tag{29}$$

$$\ln\left[A \cdot \exp\left(\frac{-E}{RT^{(j)}}\right)\right] - \left(-m_{line} \cdot \frac{1}{T^{(j)}} + n_{line}\right) = 0 \tag{30}$$

$$F_{CH_4}^{i(j)} - \left(F_{CH_4}^{o(j)} + F_{CO_2}^{o(j)} + F_{CO}^{o(j)}\right) = 0 \tag{31}$$

$$4F_{CH_4}^{i(j)} + 2F_{H_2O}^{i(j)} - \left(4F_{CH_4}^{o(j)} + 2F_{H_2O}^{o(j)} + 2F_{H_2}^{o(j)}\right) = 0 \tag{32}$$

$$F_{H_2O}^{i(j)} - \left(F_{CO}^{o(j)} + F_{CO_2}^{o(j)} + F_{H_2O}^{o(j)}\right) = 0 \tag{33}$$

$$F_{N_2}^{i(j)} - F_{N_2}^{o(j)} = 0 \tag{34}$$

where F designates the molar flow rate [mol s^{-1}], superscripts i and o represents input and output flows and subscripts describes the respective chemical species. The additional variables m_{line} and n_{line} are the Arrhenius line coefficients. All of the equations presented above are applied for the calculation of each experimental point (configuration) – the total number of equations used in the mathematical model equals $6n$, where n is the amount of experimental points.

The total number of measurement points used in the analysis was $n = 52$. Table 3 presents the vector containing the measured and unknown variables. The beginning part contains measured values (10 variables for each of the measurement points, in total 520 variables) and then the unknowns. The most important unknowns are the empirical parameters that describe the process: a, b, E and A. Moreover, the additional variables, like Arrhenius line coefficients and output flows of water, nitrogen and all components, $F_{H_2O}^{o(j)}$, $F_{N_2}^{o(j)}$ and $F_{ALL}^{o(j)}$ (defined for each measured point) are incorporated into the process model and the total number of unknowns equal to 162. Table 3 presents also the assumed errors for all the variables, which defines the covariance matrix. The uncertainties of the measured values were determined on the basis of the error analysis conducted for the respective measuring devices. In the case of the unknowns the initial errors were assumed as 100% of the initiatory values, which were determined in the preliminary calculations.

After the definition of all elements of the mathematical model was made, it was possible to apply the GLS algorithm: linearize the constraint equations, determine the Jacobi's matrix and compute the correction vectors $\mathbf{V_B}$ and new error bounds for the corrected data (covariance matrix $\mathbf{C_{VB}}$). The values of the corrected unknowns and its errors are presented in Table 4, and the corrected kinetic equation is:

$$R_{st} = w_{cat} \cdot 6.472 \times 10^{-3} \cdot \exp\left(\frac{-121 \times 10^3}{RT}\right)(p_{CH_4})^{0.88}(p_{H_2O})^{-0.083} \tag{35}$$

Table 5 presents the results obtained for one of the measurement points, and similar results can be observed in the case of all of them. It can be noted that the corrected data has smaller uncertainty than the initially assumed one. It is an effect of applying constraint equations, which provides additional information about the analysed system. The biggest improvement can be seen in the case of temperature measurement as well as in the results obtained from the gas chromatography–output flows of CH_4, H_2, CO_2 and CO.

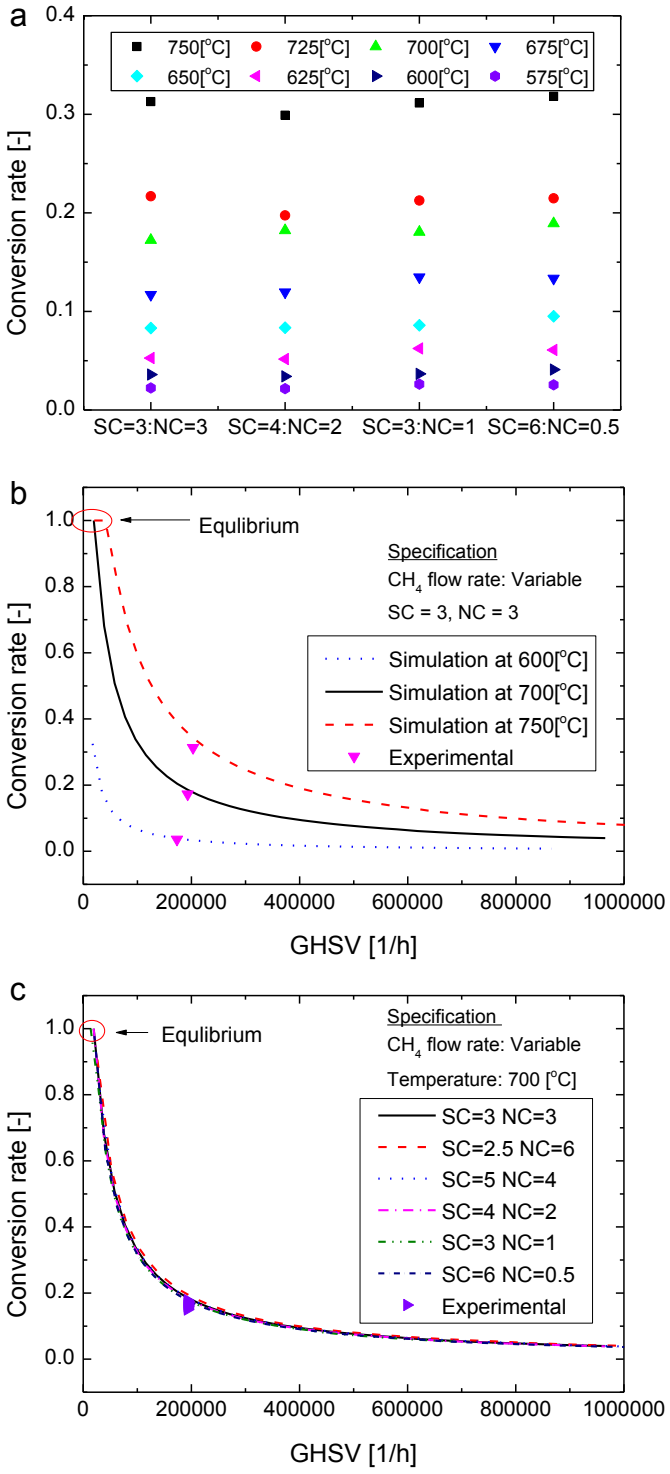

Fig. 6. Conversion rate (a) representative examples obtained from the experiment, (b) in the correlation with Gas Hourly Space Velocity (GHSV) at the condition (SC = 3 and NC = 3), (c) in the correlation with GHSV at the condition of the reaction temperature at 700[°C].

Table 3
Variables (measurements and unknowns) with assumed errors.

Index	Variable		Unit	Assumed error	Comments
Measurements – **u**					
$10 \cdot j + 1$	$T^{(j)}$	Temperature	[°C]	$\pm(2 + 0.007 \cdot T^{(j)})$	Variables for single measurement point Total number of measurement points – n $j = 0,1,\ldots,n$-1
$10 \cdot j + 2$	$w(j)$	Catalyst weight	[g]	±0.0005	
$10 \cdot j + 3$	$\Delta P^{(j)}$	Pressure	[MPa]	$\pm 0.003 \cdot \Delta P^{(j)}$	
$10 \cdot j + 4$	$F^{i(j)}_{CH_4\_v}$	CH_4 input flow	[ml min^{-1}]	$\pm 0.002 \cdot F^{i(j)}_{CH_4\_v}$	
$10 \cdot j + 5$	$F^{i(j)}_{H_2O\_v}$	H_2O input flow	[ml min^{-1}]	$\pm 0.04 \cdot F^{i(j)}_{H_2O\_v}$	
$10 \cdot j + 6$	$F^{i(j)}_{N_2\_v}$	N_2 input flow	[ml min^{-1}]	$\pm 0.002 \cdot F^{i(j)}_{N_2\_v}$	
$10 \cdot j + 7$	$m^{o(j)}_{CH_4}$	CH_4 molar fraction in products	[–]	±1	
$10 \cdot j + 8$	$m^{o(j)}_{H_2}$	H_2 molar fraction in products	[–]	±1	
$10 \cdot j + 9$	$m^{o(j)}_{CO_2}$	CO_2 molar fraction in products	[–]	±0.5	
$10 \cdot j + 10$	$m^{o(j)}_{CO}$	CO molar fraction in products	[–]	±0.5	
Unknowns – **x**					
$10 \cdot n + 1$	a	Reaction order	[–]	100% a	4 major unknowns
$10 \cdot n + 2$	b	Reaction order	[–]	100% b	
$10 \cdot n + 3$	A	Pre-exponential factor	[mol kg^{-1} s^{-1} Pa$^{-(a+b)}$]	100% A	
$10 \cdot n + 4$	E	Activation energy	[J mol^{-1}]	100% E	
$10 \cdot n + \ldots$	…	Additional unknowns	…	…	

Table 4
Analysed results – unknown variables (initial and corrected values).

Unknown	Initial value	±Initial error	Correction	Corrected value	±Corrected error
a	0.97	±0.97	0.09	0.880	±0.058
b	−0.08	±0.08	−0.163	0.083	±0.039
A	1.554×10^{-3}	$\pm 1.554 \times 10^{-3}$	-4.918×10^{-3}	6.472×10^{-3}	$\pm 1.921 \times 10^{-3}$
E	117.22×10^{3}	$\pm 17.22 \times 10^{3}$	-4.07×10^{3}	121.3×10^{3}	$\pm 2.8 \times 10^{3}$

The improvement obtained by the use of the GLS algorithm can be seen clearly by comparison of the residuum of the model equations w_j solved with the initial and corrected data. For the kinetic reforming equation in Eq. (29), the sum of the residuum for all measurement points before the application of the GLS algorithm is 1.4×10^{-2} and after data correction it is 9.798×10^{-4}. Similar dependence can be observed in the case of other equations – the sum of the residuum for all equations applied to all the measurement points is 11.47 before the application of the GLS algorithm and 3.70 after.

5. Conclusions

The present paper highlighted the challenge in the study of reaction kinetics derived in the methane/steam reforming process with a novel approach combining the Orthogonal Least Squares mathematical methodology. A calculation procedure incorporating the Generalized Least Squares (GLS) method has been proposed to estimate the basic parameters of the methane/steam reforming kinetics over the Ni/YSZ, typically used for SOFC anodic catalytic material. The introduced mathematical model has been based only on the fundamental physical equations describing the chemical process, and it can be noted that it does not contain any additional assumptions in accordance with the precise stoichiometry of the occurring reactions. This property provides the greater versatility to the proposed methodology in comparison with approaches used in the previous studies.

Three main phases of the conducted research can be pointed: the experimental investigation of the methane/steam reforming process over a fine powder catalyst of NiO/YSZ after reduction, the numerical analysis of collected data which aimed to find the initial approximations of empirical parameters describing the process, and finally the application of the GLS algorithm.

The method proposed in the present paper not only allows to obtain the most probable values of the estimated parameters but also makes possible the *a posteriori* evaluation of the errors of directly measured variables and unknown parameters. It was demonstrated that the GLS method is useful in securing higher accuracy of measured data and decreasing the value of residuum of constraint equations. The present results primarily proved an applicability of the GLS methodology into the investigation of a chemical reaction process for deriving its reaction kinetics. Moreover, it can be noted that the GLS method has the potential to provide the objective criteria for the formal evaluation and falsification of different mathematical models of the methane reforming process. Furthermore, the proposed algorithm can be easily adapted to the mathematical modelling of the fuel reforming process for different catalysts and experimental conditions. This approach can clarify the divergence between the published contradictory results about the reaction kinetics' parameters. The

Table 5
Analysed results – variables for one of the measurement point (initial and corrected values).

Variables	Initial value	±Initial error	Correction	Corrected value	±Corrected error
T	700	±2.49	−0.004	700.00	±0.36
w	1.887	$\pm 5.0 \times 10^{-4}$	1.08×10^{-6}	1.887	$\pm 5.0 \times 10^{-4}$
ΔP	5.0×10^{-3}	$\pm 1.50 \times 10^{-5}$	7.85×10^{-9}	5.00×10^{-3}	$\pm 1.50 \times 10^{-5}$
$F^{i}_{CH_4\_v}$	35	±0.07	-4.6×10^{-4}	35.000	±0.070
$F^{i}_{H_2O\_v}$	0.13	$\pm 5.2 \times 10^{-3}$	-8.9×10^{-4}	0.1309	$\pm 5.1 \times 10^{-3}$
$F^{i}_{N_2\_v}$	140	±0.28	1.11×10^{-17}	140	±0.28
$m^{o}_{CH_4}$	18.328	±1	0.6171	17.71	±0.70
$m^{o}_{H_2O}$	14.553	±1	−0.4787	15.03	±0.75
$m^{o}_{CO_2}$	3.257	±0.5	−0.0037	3.26	±0.33
m^{o}_{CO}	0.532	±0.5	−0.1353	0.67	±0.38

authors of the present paper strongly believe that the application of the GLS method can provide a great benchmark in the evaluation of the reaction process and qualify the level of mathematical modelling of reaction processes.

Acknowledgements

This work was supported by the Polish National Centre for Research and Development (Project HTRPL, Contract No. SP/J/1/166183/12) and the Precise Measurement Technology Promotion Foundation of Japan.

References

[1] K. Eguchi, H. Kojo, T. Takeguchi, R. Kikuchi, K. Sasaki, Solid State Ionics 153 (2002) 411.
[2] G. Brus, Int. J. Hydrogen Energy 37 (2012) 17225.
[3] D. Mogensen, J.-D. Grunwaldt, P.V. Hendriksen, K. Dam-Johansen, J.U. Nielsen, J. Power Sources 196 (2011) 25.
[4] J. Xu, G.F. Froment, AIChE J. 35 (1989) 97.
[5] J. Wei, E. Iglesia, J. Catal. 225 (2004) 116.
[6] E. Achenbach, E. Riensche, J. Power Sources 52 (1994) 283.
[7] K. Ahmed, K. Foger, Catal. Today 63 (2000) 479.
[8] G. Brus, Y. Komatsu, S. Kimijima, J.S. Szmyd, Int. J. Thermodyn. 15 (2012) 43.
[9] H. Iwai, M. Ueda, T. Takahashi, M. Saito, H. Yoshida, in: Proc. 8th Int. Symp. Heat Transf., Beijing, 2012. ISHT–8–06–1, 1–8.
[10] D. King, J. Strohm, X. Wang, H. Roh, C. Wang, Y. Chin, Y. Wang, Y. Lin, R. Rozmiarek, P. Singh, J. Catal. 258 (2008) 356.
[11] A.L. Lee, R.F. Zabransky, W.J. Huber, Ind. Eng. Chem. Res. 29 (1990) 766.
[12] R. Odegard, E. Johnsen, H. Karoliusen, in: M. Dokiya, O. Yamamoto, H. Tagawa, S.C. Singhal (Eds.), Proc. 4th Int. Symp. Solid Oxide Fuel Cells, ECS, Yokohama, Japan, 1995, pp. 810–819.
[13] H. Timmermann, D. Fouquet, a. Weber, E. Ivers-Tiffée, U. Hennings, R. Reimert, Fuel Cells 6 (2006) 307.
[14] J. Xu, G.F. Froment, AIChE J. 35 (1989) 88.
[15] H. Yakabe, T. Ogiwara, M. Hishinuma, I. Yasuda, J. Power Sources 102 (2001) 16.
[16] D. Mogensen, Methane Steam Reforming Kinetics over Ni-YSZ Anodematerials for Solid Oxide FuelCells Methane Steam Reforming Kinetics Over Ni-YSZ Anode Materials for Solid Oxide Fuel Cells, Technical University of Denmark, 2011.
[17] A.-M. Legendre, Nouvelles Méthodes Pour La Détermination Des Orbites Des Comètes, F. Didot, Paris, 1805.
[18] A.G. Swenker, Acta IMEKO 29 (1964).
[19] Z. Kolenda, J. Allman, Bull. l'Academie Pol. Sci. 22 (1974) 6.
[20] Z. Kolenda, J. Szmyd, Arch. Metall. Mater. 3 (1985) 3.
[21] J. Szargut, Z. Kolenda, K. Taramin, Energy Res. 5 (1981) 253.
[22] Z. Kolenda, J. Szmyd, S. Slupek, L. Baez, Can. J. Chem. Eng. 61 (1983) 627.
[23] J. Szmyd, K. Suzuki, Z. Kolenda, J. Humphrey, JSME Int. J. Ser. II 35 (1992) 599.
[24] Z. Kolenda, J. Szmyd, K. Dziedziniewicz, Arch. Metall. Mater. 32 (1987) 587.
[25] Z. Kolenda, J. Donizak, J. Bocardo, Metall. Mater. Trans. B 30B (1999) 505.
[26] Z. Kolenda, Z. Zembura, J. Donizak, M. Zembura, J. Electroanal. Chem. 382 (1995) 1.
[27] E.K. Mikhail, F.E. Ackermann, Observations and Least Squares, IEP, New York, 1976.
[28] S. Brandt, Statistical and Computational Methods in Data Analysis, North-Holland Publishing Company, Amsterdam, 1970.
[29] AGC Semi Chemical Co. Ltd., Catalyst Analysis Sheets, 2009.
[30] N.F.P. Ribeiro, M.M.V.M. Souza, O.R.M. Neto, S.M.R. Vasconcelos, M. Schmal, Appl. Catal. A Gen. 353 (2009) 305.
[31] K. Wincewicz, J. Cooper, J. Power Sources 140 (2005) 280.
[32] S.P. Jiang, S.H. Chan, J. Mater. Sci. 39 (2004) 4405.
[33] F.H. Wang, R.S. Guo, Q.T. Wei, Y. Zhou, H.L. Li, S.L. Li, Mater. Lett. 58 (2004) 3079.
[34] M.A. Vannice, Kinetic of Catalytic Reactions, Springer, New York, 2005.
[35] N. Itoh, W. Yu, J. Jpn. Inst. Energy 85 (2006) 307.